Studying the effect of the tracking system on the solar collector

Mohammed Younus Ammar Alhamd	Department of Mechanical Engineering, University of Mosul, Nineveh, Iraq, m.y.ammaralrawi@gmail.com
Ammar Younis Ibrahim Alrawy	Department of Mechanical Engineering, University of Mosul, Nineveh, Iraq, drammar2020@uomosul.edu.iq
Ziad Shakeeb Alsarraf	Department of Mechanical Engineering, University of Mosul, Nineveh, Iraq, ziadalsarraf@uomosul.edu.iq

ABSTRACT

With the development of the utilization of solar radiation to obtain thermal energy, the types of systems extracted for this energy increased, most notably the parabola solar collector. The parabola was designed precisely by the SOILDWORKS program and the case was simulated by the ANSYS CFD program, which represents the entry of water with a mass flow rate of 100 ml and a temperature of 22 degrees Celsius, adding the longitude, latitude, day and hour in the data and calculating the amount of solar radiation in two cases of the solar collector. With the tracking system and without it, and calculating the external and internal energy to know the improvement of the efficiency of the system. Water entering the solar collector acquires the greatest amount of thermal energy. Hottest temperature recorded on the first day had risen to 58°C at 14:30. The tracking system proved helpful in following the sun's beams and collecting the highest quantity of energy released by the sun when the inlet temperature was 25°C.

Keywords: Solar collector, Tracking system, Numerical calculation, CFD, FEM, Parabolic solar collector, Thermal efficiency

1.Introduction

In this study, a distributed collector field called ACUREX at the PSA (Solar Plant of Almer'a) solar power plant is used to a robust model predictive control (RMPCT) for tracking of piece-wise constant references. A solar power plant's fundamental feature is its inability to control its principal energy source, solar radiation. The intensity of solar radiation fluctuates during the day, changing plant dynamics and significantly disrupting the process [1]. The hardware design and execution of a system that assures a solar panel's perpendicular profile with the sun in order to capture the most energy from the sun's rays is presented in a paper. With the suggested system in place, an extra 25 to 30 percent of energy is created, with the system itself using relatively little of it [2]. The development of a parabolic trough solar collector with a 24:1 concentration ratio. Dual-axis tracking had an optical efficiency of 0.813 percent, which was greater than the tracking modes of east-west and north-south by 14.3 percent and 40.9 percent, respectively [3]. The suggested two-axis Sun tracking system was distinguished by a relatively easy-to-install, low-cost electromechanical setup with little maintenance needs. According to the findings, the measured solar energy gathered on

the moving surface was much more (up to 46.46 percent) than on the stationary surface [4]. The sun tracking formula in its broadest sense, which encompasses all potential on-axis tracking techniques, is described. It can provide a general mathematical solution, but more importantly, by addressing the solar collector placement mistake, it may increase the accuracy of solar tracking [5]. The stainless-steel parabolic reflector, the flat solar receiver, the thermal storage tank, and the closed-loop tracking system make up the parabolic trough solar collector. The tracking system is made up of electromechanical parts such a gearbox, control box, DC motor, and picture sensor. The tracking devices are powered by a compact power unit that consists of two solar panels and a 12 V battery. The device has been used as a demonstration unit in practical thermal science courses covering topics like renewable energy. Students' comprehension of renewable energy sources and processes is improved by this kind of practice [6]. Solar collector, tracking PV array, battery bank, microcontroller, and DC converter make up the system. It is envisaged that this design would be a suitable method for supplying solar radiation energy to provide the best outcome. This work presents the experimental results of the voltage and power response in arranging the PV to produce a solar drying system device with the highest possible photovoltaic array output power [7]. Process heat generated by solar collectors may greatly aid in the preservation of traditional energy sources, the reduction of CO2 emissions, and the postponement of global warming. The system temperature fluctuation that occurs under unsteady-state radiation circumstances is one of the main issues with the use of solar process heat. System functioning is unaffected by brief radiation instability intervals of less than 30 minutes [8]. Water or air may be heated using a solar collector. If it faces the sun all the time, its efficiency will rise. However, it implies that a tracking system is necessary. The ideal tilt angle for putting a solar collector is the angle at which the solar radiation will strike the surface perpendicularly, and this study is done to assist the farmers [9]. The goal of the project is to create a simple, reasonably priced solar tracker system with two axes (azimuth angle and altitude angle), utilizing a real-world Light Dependent Resistor (LDR). A solar panel, a two-motor satellite dish and ball-joint, an LDR sensor module, and an electrical circuit make up the project. The findings of this project's comparison with fixed solar panels indicated that solar trackers produce more electricity than fixed solar panels [10]. A possible approach for producing scalable solar energy is solar power concentration. In order to concentrate solar electricity, concentrated sunlight must be converted into heat. The yearly average efficiency of the commercial parabolic trough collector is now at 50%, and cosine loss is mostly to blame for this low efficiency. The daily average efficiency may be raised from 43% to 48% in winter using rotatable axis tracking [11]. The observed temperatures on the absorbing surfaces and the values of the incoming solar radiation recorded with a fixed and a sun-tracking pyranometer indicate a satisfactory correlation in spherical shape and flat plate absorber exposed to sun without cover. A thermal camera has been used to investigate temperature dispersion. The spherical absorber may not be an effective solar radiation catching surface since its daily average temperature is lower than that of a flat plate [12]. In this study, an experimental investigation of a linear Fresnel lens-based concentrating solar collector is presented. The thermal efficiency of this solar collector is predicted to be greater than that of flat-plate or evacuated tube solar collectors at a comparatively high temperature. According to experimental findings, it has a conversion efficiency of roughly 50% when the water temperature is 90 °C and 0.578 W/m2 K when the temperature is 200 °C [13]. It is crucial to employ

a sun tracker with sufficient precision even if the accuracy of one used in household hot water solar collectors is not yet standardized. Despite having excellent quality, the concerned tractor would have large optical losses since the sun radiation couldn't be focused properly onto its receiver [14]. To calculate the performance of SUPP based on tracking solar collector consideration in Malaysia, a mathematical model was created. Experimental work was used to validate the model, and good agreement was attained. Results showed that SUPP with a slope collector angle of 10 may generate more electricity throughout the whole year. Additionally, compared to a red collector, the tracking solar consideration improved performance characteristics by around 3.5 KW [15]. An essential part of parabolic trough solar thermal power generating systems is the parabolic trough collector. The circumferential flux distribution on absorber tubes was simulated using coordinate transformations and the Monte Carlo Ray Trace (MCRT) technique. The geometric concentration ratios (GCs), the glass tube transmissivity, the absorber tube absorptance, and the collector surface reflectivity are all included in the simulation model. The X-direction installation error is 0.2 percent 0.2 percent, the Y-direction tracking error is 1.0 percent e 0.5 percent, and the tracking error should be less than 4 mrad for a GC of 20 and a 90-degree rim angle [16].

2.Methodology

The process of designing the parabola and water transfer pipes was done by SOLIDWOKS program as in Figure (1).

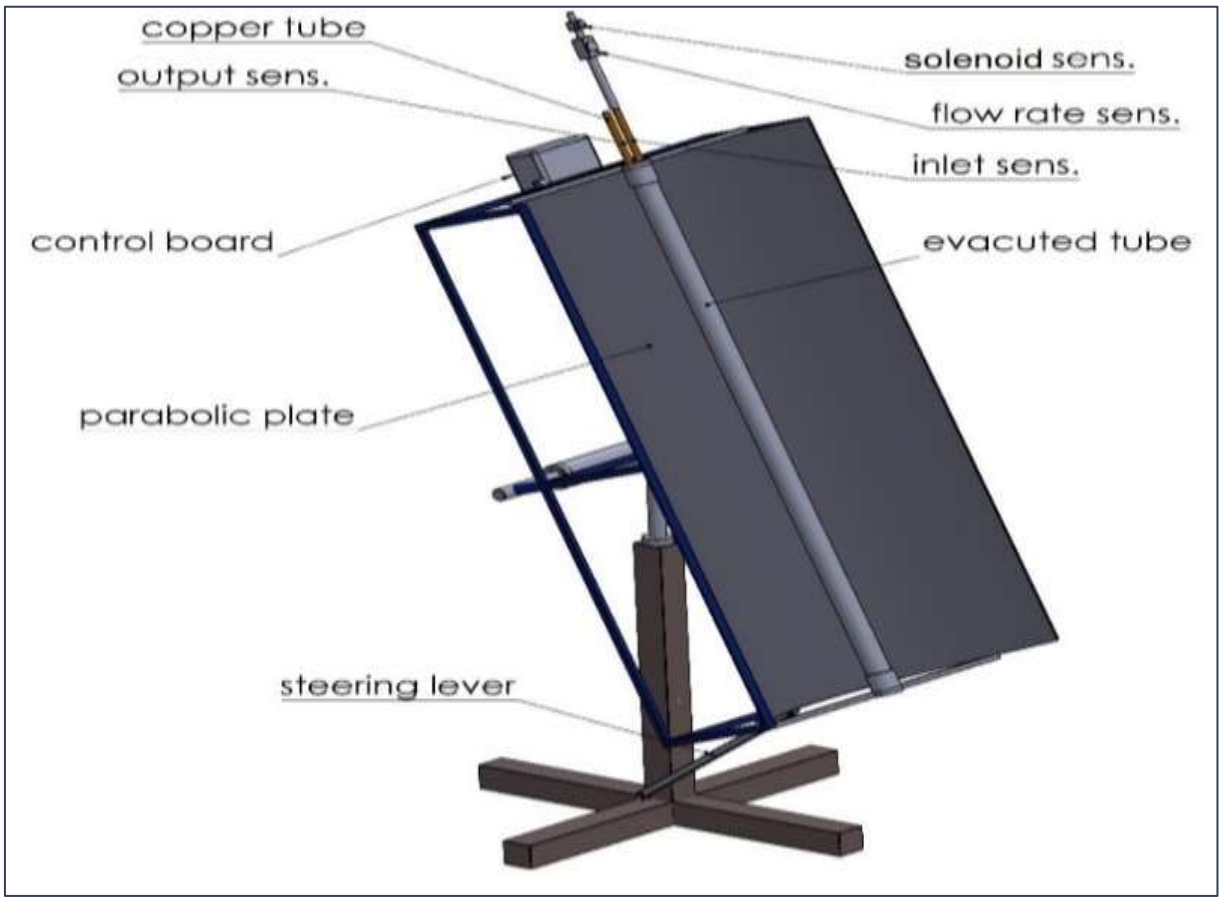

(a)

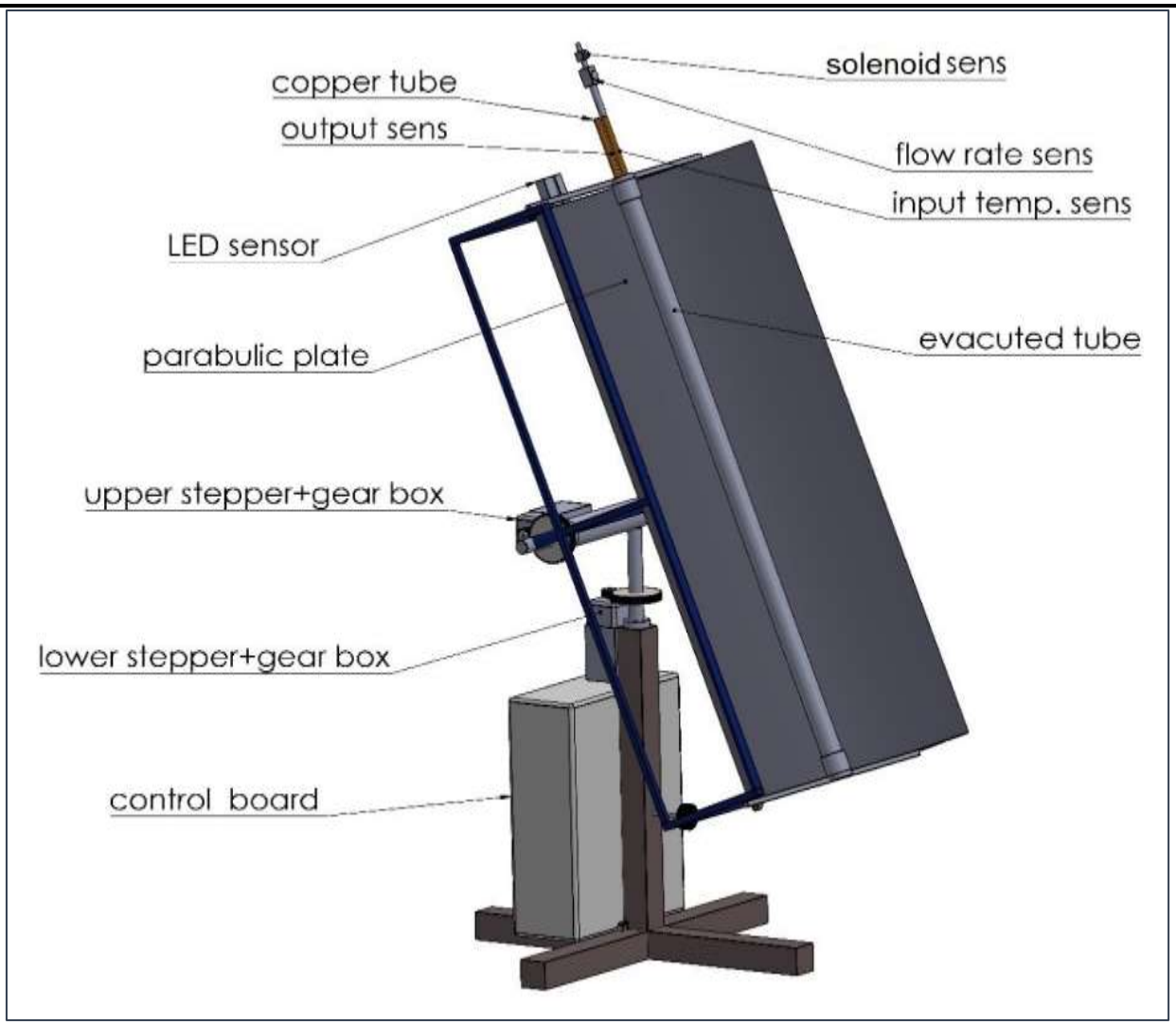

(b)

Figure (1): geometry of solar collector. (a) without tracking system, (b) with tracking system.

Where the parabola was simulated by the ANSYS CFD program, which specializes in heat transfer and fluid movement, taking into account the precise mesh to obtain the accurate results.

The governing equations that were used in the data:

The radiative transfer equation (RTE) in the direction is taken into account by the DO model as a field equation. Equation 1 is so written as

$$\nabla \cdot (I(\vec{r},\vec{s})\vec{s}) + (a+\sigma_s)I(\vec{r},\vec{s}) = an^2\frac{2T^4}{\pi} + \frac{\sigma_s}{4\pi}\int_0^{4\pi} I(\vec{r},\vec{s}')\Phi(\vec{s}\cdot\vec{s}')d\Omega' \dots\dots\dots\dots\dots 1$$

Ansys Fluent also allows the modeling of non-gray radiation using a gray-band model. The RTE for the spectral intensity $I_\lambda(\vec{r},\vec{s})$ can be written as equation 2

$$\nabla \cdot (I_\lambda(\vec{r},\vec{s})\vec{s}) + (a_\lambda + \sigma_s)I_\lambda(\vec{r},\vec{s}) = a_\lambda I_{b\lambda} + \frac{\sigma_s}{4\pi}\int_0^{4\pi} I_\lambda(\vec{r},\vec{s}')\Phi(\vec{s}\cdot\vec{s}')d\Omega' \ldots\ldots\ldots 2$$

Here, $I_{b\lambda}$ is the blackbody intensity determined by the Planck function, I_λ λ is the spectral absorption coefficient, and λ is the wavelength. It is assumed that the scattering coefficient, scattering phase function, and refractive index are wavelength-independent. The non-gray DO implementation separates the radiation spectrum into wavelength bands, which are not required to be continuous or of the same size. The wavelength intervals that you provide (n=1) are equivalent to values in vacuum. The radiant energy contained in each wavelength band is calculated using the RTE and integrated across each wavelength interval to provide transport equations. Each band's conduct is considered to be gray. The formula for the black body emission in the wavelength band at one solid angle is

$$[F(0 \to n\lambda_2 T) - F(0 \to n\lambda_1 T)]n^2\frac{\sigma T^4}{\pi} \ldots\ldots\ldots\ldots\ldots\ldots 3$$

where F(0→nλT) is the fraction of radiant energy emitted by a black body [419] in the wavelength interval from 0 to λ at temperature T in a medium of refractive index n.λ_2 and λ_1 are the wavelength boundaries of the band.

The total intensity I(r ⃗,s ⃗) in each direction S ⃗ at position r ⃗ is computed using

$$I(\vec{r},\vec{s}) = \sum_k I_{\lambda_k}(\vec{r},\vec{s})\Delta\lambda_k \ldots\ldots\ldots\ldots\ldots\ldots 4$$

when the wavelength bands are added together. The non-gray DO model's boundary conditions are implemented on a band basis. Similar to how the gray DO model is treated inside bands.

The finite volume radiative heat transfer system accelerates convergence due to the link between energy and radiation intensities at a cell. With this technique, the convergence for situations requiring optical thicknesses higher than 10 is significantly improved. This often happens in applications that melt glass. When scattering is considerable, this characteristic benefits from the high connection between directional radiation intensities. By selecting the DO/Energy Coupling option for the DO model in the Radiation Model dialog box, this DO model implementation in Ansys Fluent may be used. The following list contains the coupled method's discrete energy equations. The discrete energy equation is produced by integrating the energy equation across a control volume.

$$\sum_{j=1}^{N}\mu_{ij}^T T_j - \beta_i^T T_i = \alpha_i^T \sum_{k=1}^{L} I_i^k \omega_k - S_i^T + S_i^h \ldots\ldots\ldots\ldots\ldots\ldots 5$$

Where:

$\alpha_i^T = \kappa\Delta V_i$

$\beta_i^T = 16\kappa\sigma T_i^{*3}\Delta V_i$

$S_i^T = 12\kappa\sigma T_i^{*4}\Delta V_i$

$K =$ absorption coefficient

ΔV control volume

The discretization of the convection, diffusion, and non-radiative source terms is what causes the coefficient _ijT and the source term S ih. Combining Equation 1's discretized form with Equation 5's discretized energy equation results in:

$$\vec{P}_i\vec{q}_i + \vec{r}_i = 0$$

Where:

$$\vec{q}_i = \begin{bmatrix} I_i^1 \\ I_i^2 \\ \vdots \\ \vdots \\ I_i^L \\ T_i \end{bmatrix} \ldots\ldots\ldots\ldots\ldots 6$$

$$\vec{P}_i = \begin{bmatrix} M_{ii}^1 + \eta_i^{11} + \gamma_i^1\omega_1 & \eta_i^{12} + \gamma_i^1\omega_2 & \dots \beta_i^1 \\ \eta_i^{21} + \gamma_i^2\omega_1 & M_{ii}^2 + \eta_i^{22} + \gamma_i^2\omega_2 & \dots \beta_i^2 \\ \vdots & & \\ \vdots & & \\ -\alpha_i^T\omega_1 & -\alpha_i^T\omega_2 & \dots M_{ii}^T \end{bmatrix} \dots\dots\dots\dots\dots\dots 7$$

$$\vec{r}_i = \begin{bmatrix} \sum_{j=1,i\neq j}^{N} \mu_{ij}^l I_j^l - S_i^1 - S_i^B \\ \vdots \\ \vdots \\ \sum_{j=1,i\neq j}^{N} \mu_{ij}^T T_j + S_i^T + S_i^h \end{bmatrix} \dots\dots\dots\dots\dots\dots 8$$

The solar radiation falling on the parabola was entered by the latitude and longitude of the city of Baghdad, and the month and day were entered, which represents the month of March on the 28th from eight in the morning until five in the evening, which represents the time in which the sun's rays are present in a large way, where the comparison was made between the solar complex without the system Tracking with which tracking system has.

3.Results and discussion

the 28th day of March to the 20th day of April from 08:00 until 17:00. The highest temperature in a condition without the tracking system on the first day is 40.5°C at 14:30. Where the inlet temperature was 25°C with the tracking system. Noticed that the highest temperature recorded on the first day has increased to 58°C at14:30. Where at the same inlet temperature, conclude the usefulness of the tracking system in tracking the sun's rays and collecting the largest amount of radiation emitted from the sun. The water entering the solar collector obtains the largest amount of thermal energy as a result of the continuous feeding of the solar system from the sun through its movement. The numerical result from the data of the experimental work, the cases of the solar collector were simulated without and with the tracking system, where a group of cases representing numerical work was taken, which were five dates (3/28, 4/4, 4/9, 4/15, 4/20) and for three times daily in the morning, which represents the 08:00, afternoon which represents the 13:00, and the evening which represents 17:00. A comparison was made between the experimental and numerical results for these times. This is because the water entering the solar collector obtains the more of thermal energy as a result of the continuous feeding of the solar system from the sun in tracking system.

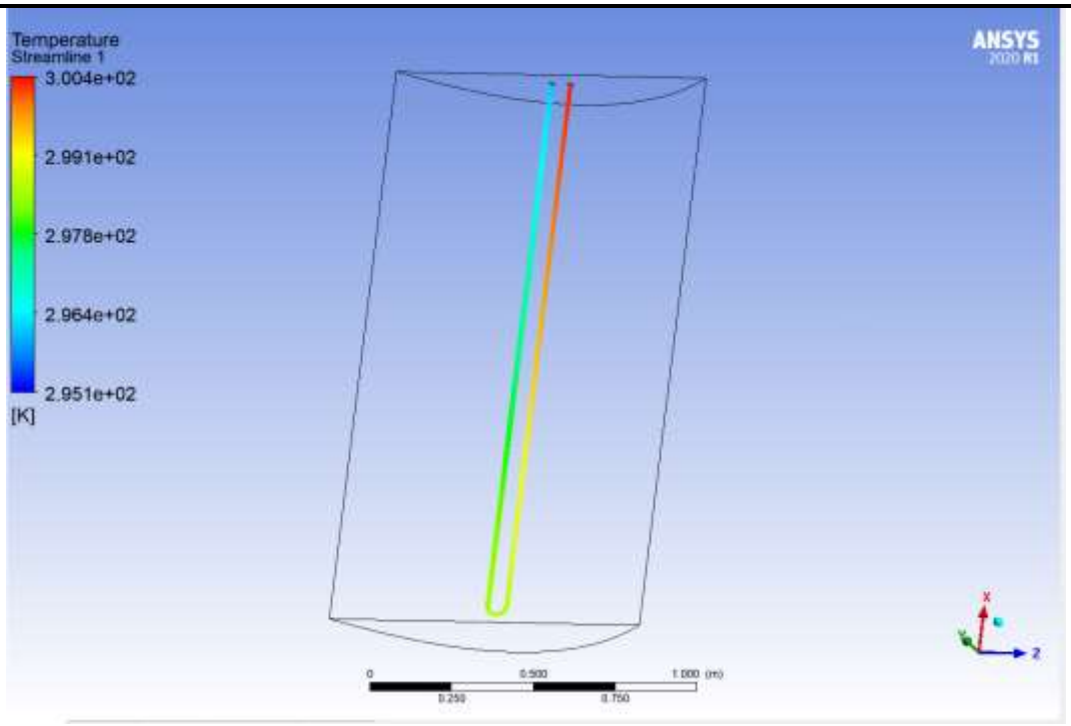
Temperature
Streamline 1
3.004e+02
2.991e+02
2.978e+02
2.964e+02
2.951e+02
[K]
ANSYS
2020 R1
0
0.500
1.000 (m)
0.250
0.750
X
Z

(a)

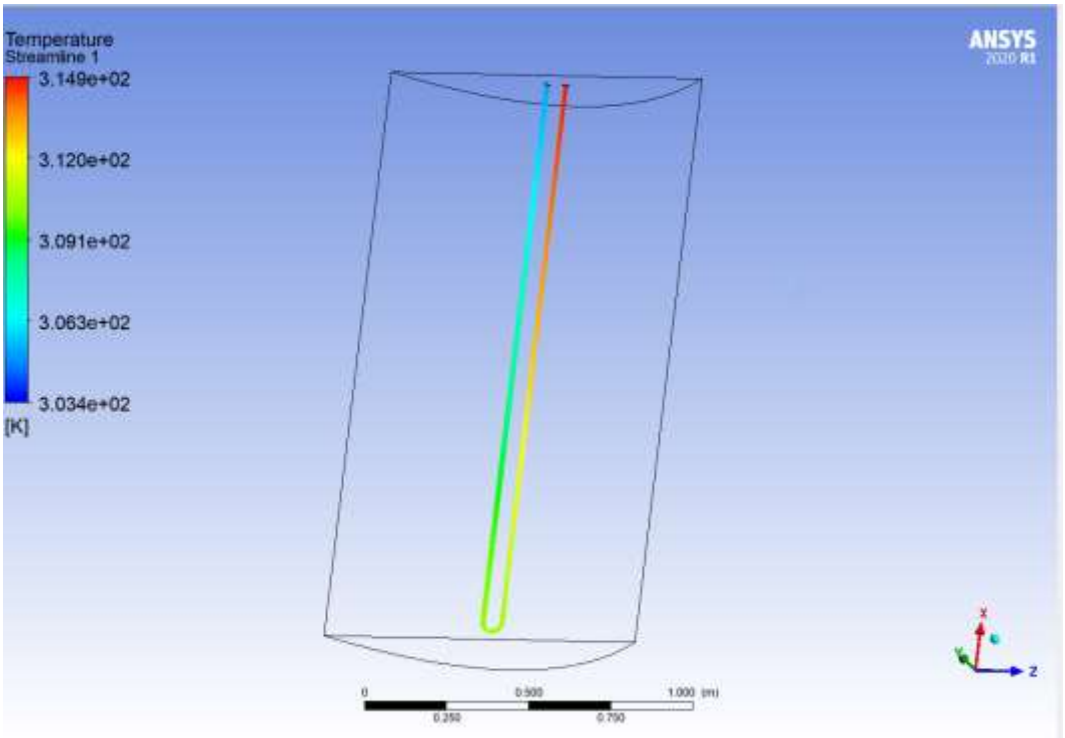
Temperature
Streamline 1
3.149e+02
3.120e+02
3.091e+02
3.063e+02
3.034e+02
[K]
ANSYS
2020 R1
0
0.500
1.000 (m)
0.250
0.750
X
Z

(b)

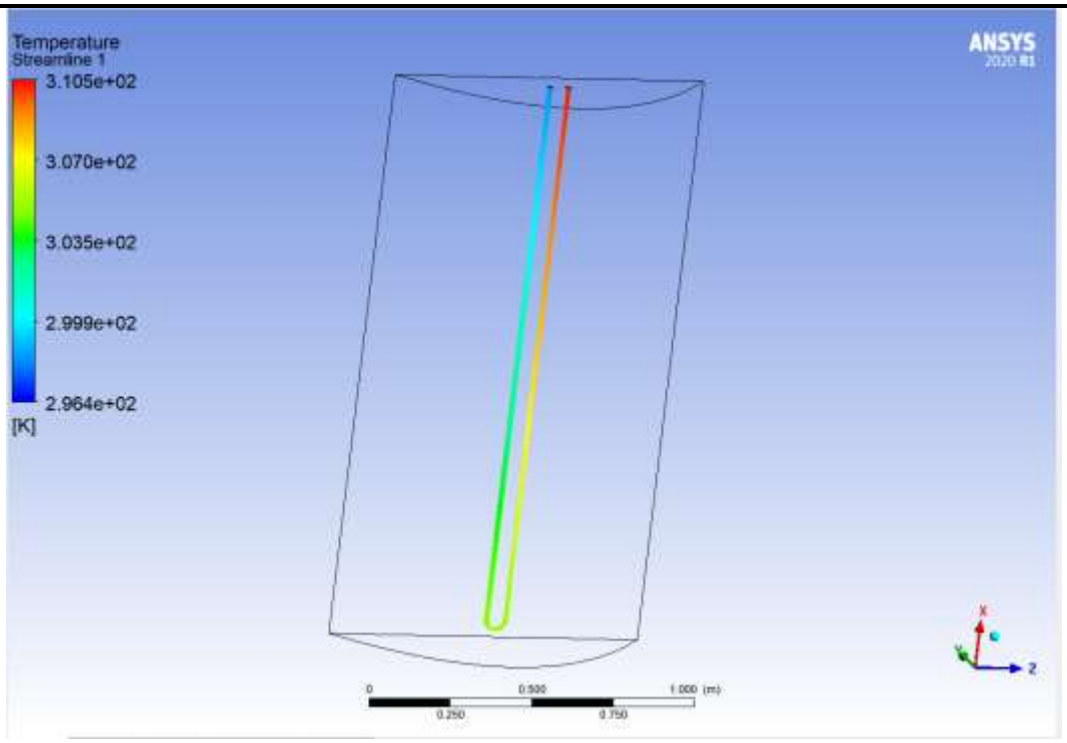

(c)

Figure (5) Temperature distribution without tracking system. (a) a.m., (b)noon, (c)p.m.

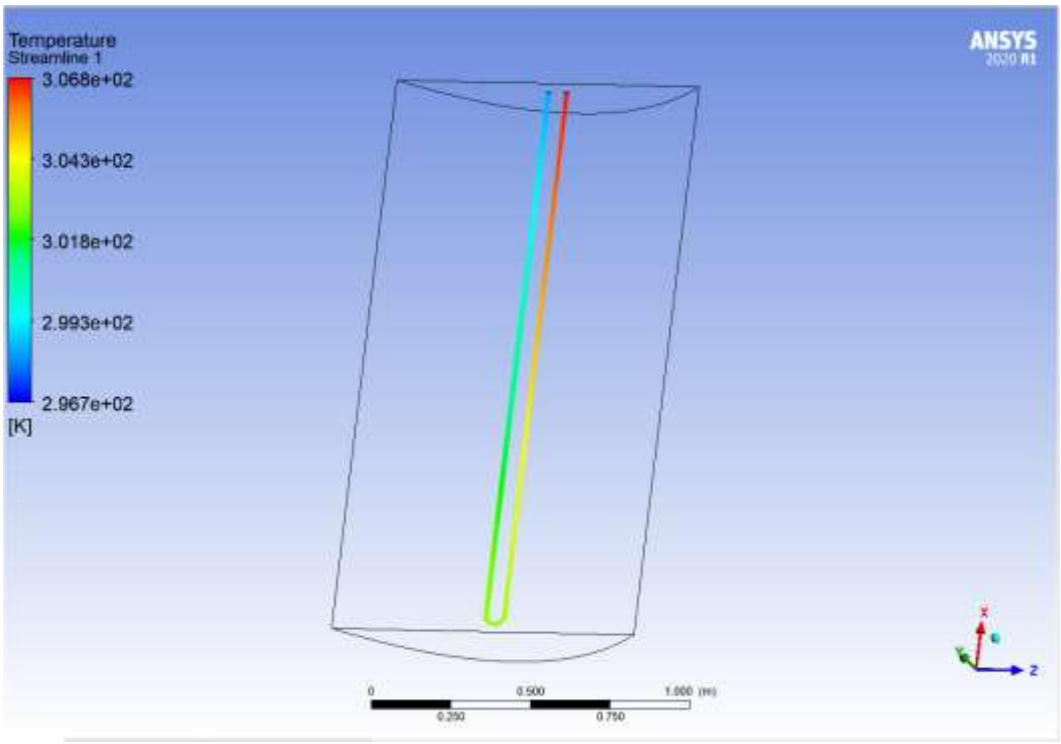

(a)

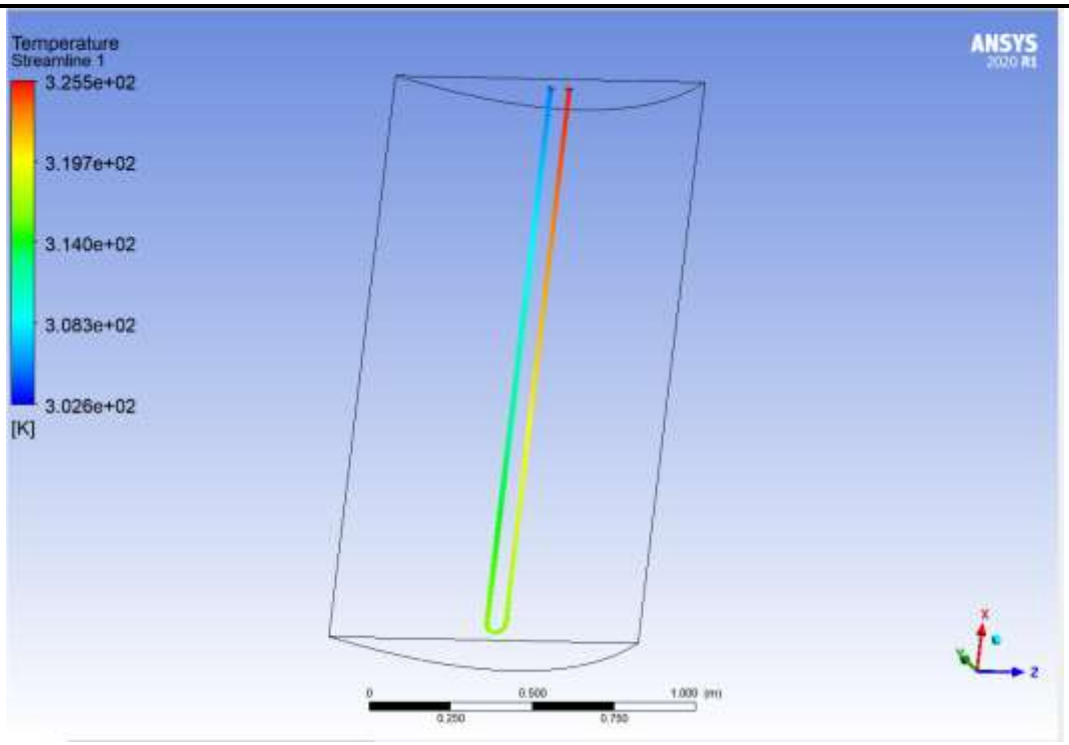

(b)

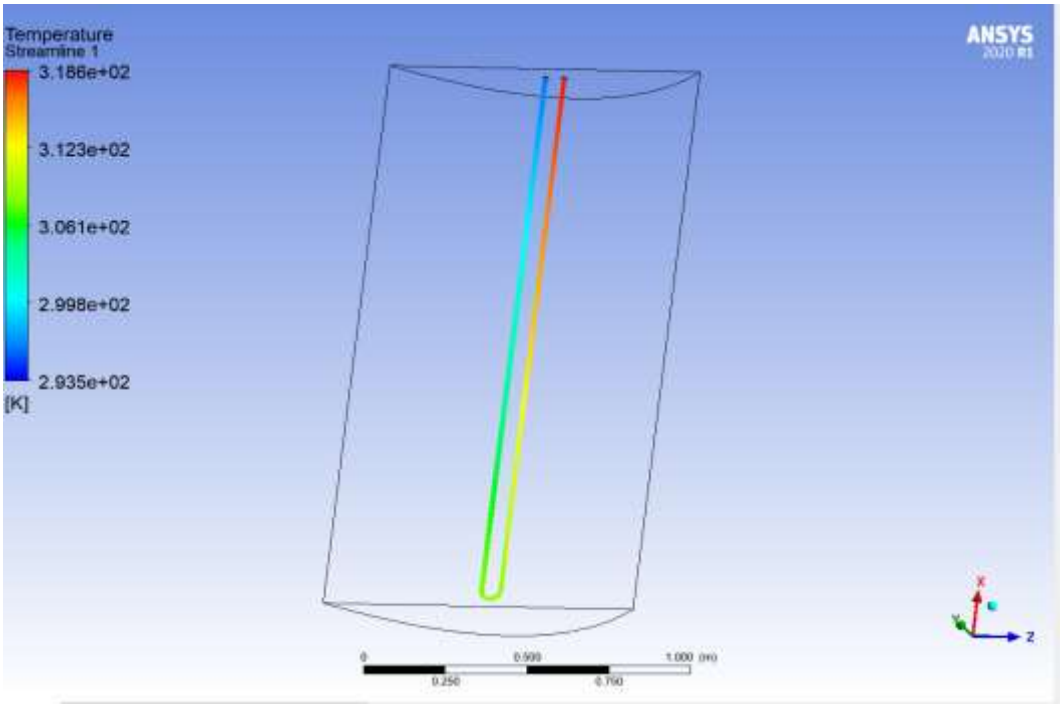

(c)

Figure (6) Temperature distribution with tracking system. (a) a.m., (b)noon, (c)p.m.

From the figures above it was noted that the temperature of the water leaving the solar collector with the presence of the tracking system compared to the solar collector without tracking system. In order to check the efficiency of the system, it is necessary to know the amount of solar radiation falling on the solar collector and knowing its effect on the temperature leaving the solar collector, as the quantities of incoming solar radiation were taken from the online ANSYS program after setting the longitude, latitude, day, months of the year and the direction of the sun's rays within the ANSYS program. The amount of heat energy transferred to the solar collector is calculated, as the amount of heat energy reserved from the solar collector at 13:00 reached its maximum 1142 w/m^2 at 3/28.

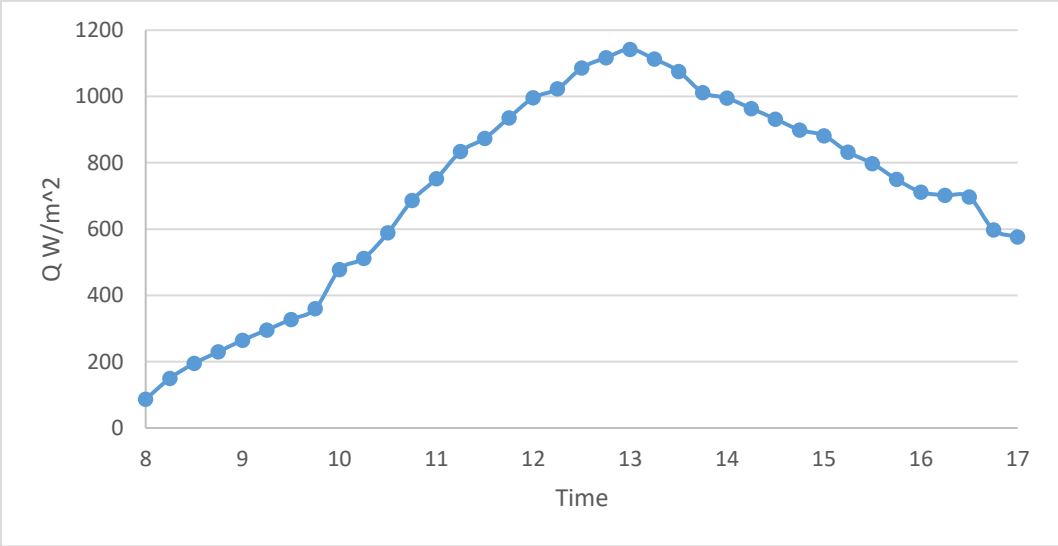

Figure (12) solar radiation on the collector with time.

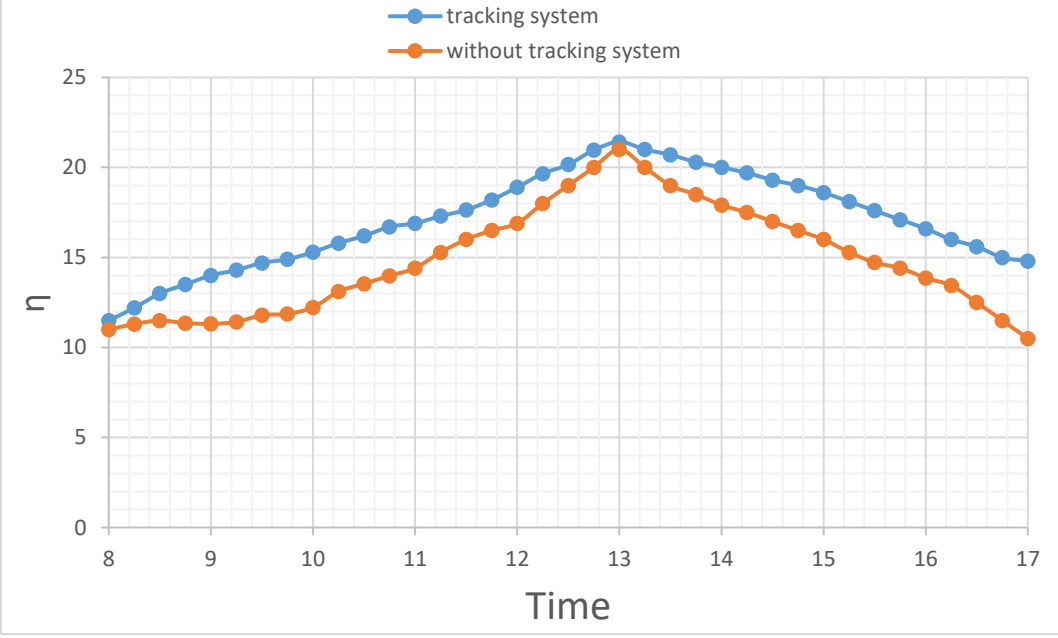

Figure (13) Thermal efficiency between the solar collector without the tracking system and the contains the tracking system.

By calculating the concentrated solar energy and its transmission to the heat energy acquired through the working fluid (water) and calculating the energy received by the water from the collector tube from the incoming and outgoing temperatures and the amount of flow to calculate the efficiency of the solar collector. Deduce the effectiveness of the tracking system which obtained more thermal energy compared to the solar collector without the tracking system. The amount of thermal energy transmitted by the incident radiation was calculated, the thermal energy was obtained, it was 1672 watts at 13:00 (3/28) by the Solar collector with tracking system.

The main work of the solar collector is to reflect the incoming solar radiation onto the tube in which the water flows and heats it, and the concentration of the incoming solar radiation greatly affects the heating of the running water in the tube. It is noted through the simulation that took place for the solar collector without the tracking system and with the presence of a tracking system tracking. The amount of incident radiation to the solar collector with the tracking system reached 1142 w/m^2, while in the collector without the tracking system, the amount of incident radiation reached 1091 w/m^2 at 13:00 (3/28), where notice the difference between the amount of radiation falling between the two systems.

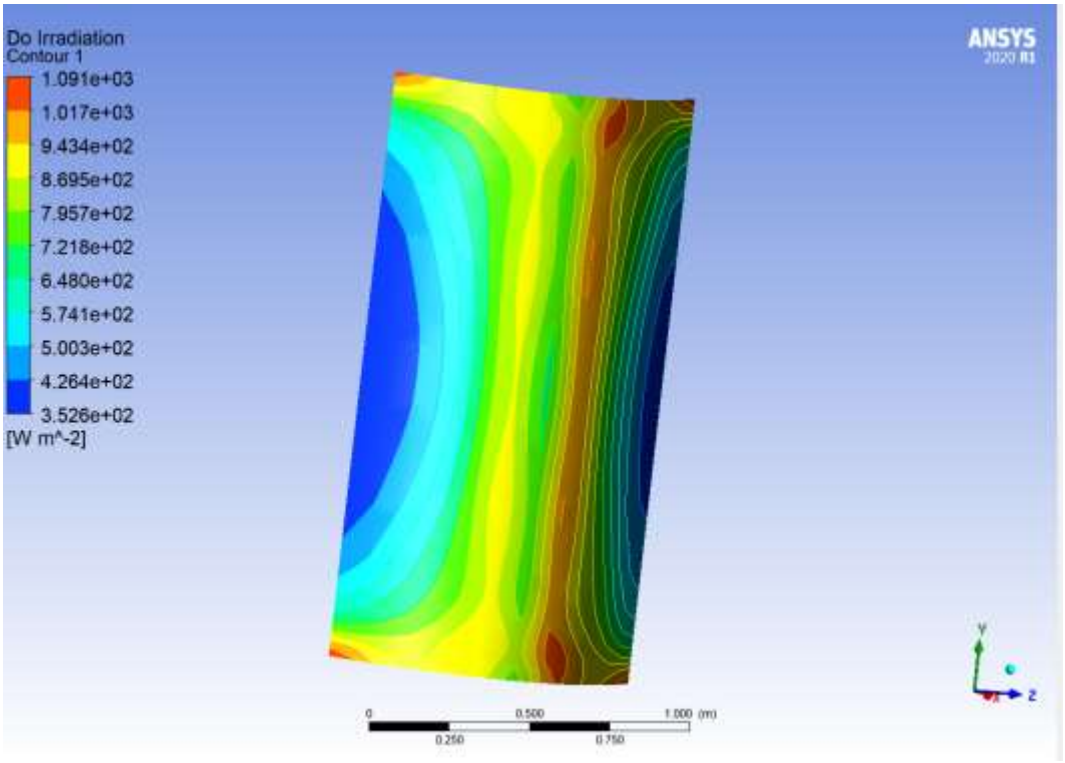

(a)

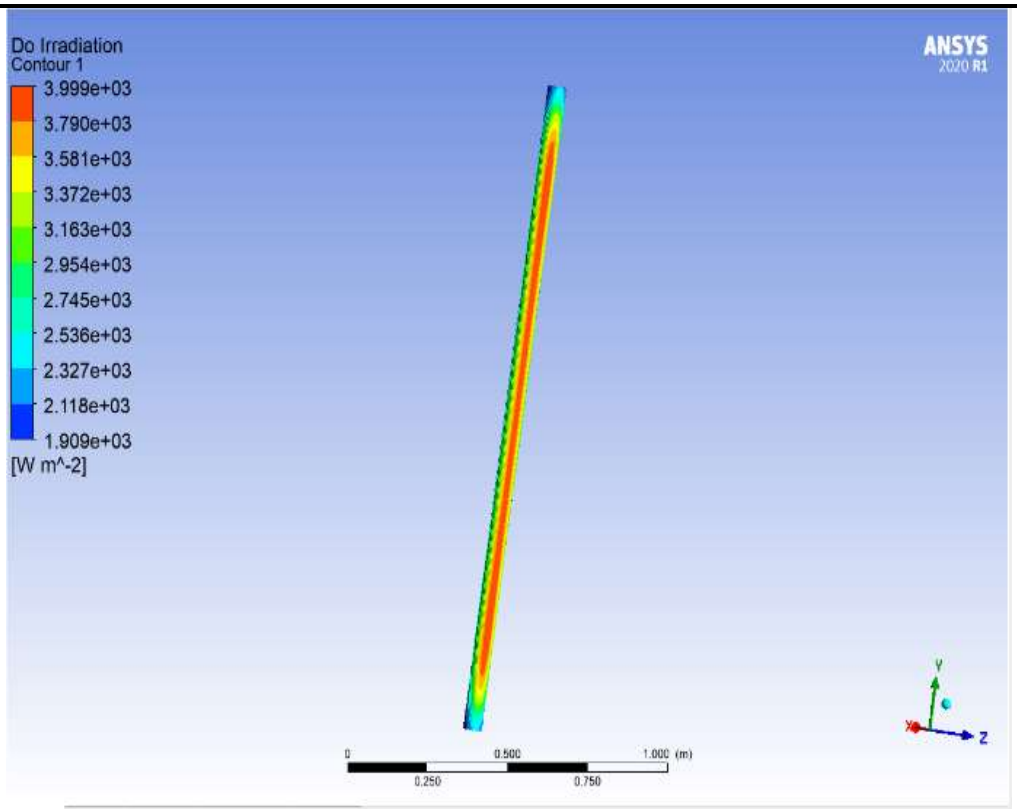
Do Irradiation
Contour 1
3.999e+03
3.790e+03
3.581e+03
3.372e+03
3.163e+03
2.954e+03
2.745e+03
2.536e+03
2.327e+03
2.118e+03
1.909e+03
[W m^-2]
ANSYS
2020 R1
0
0.500
1.000 (m)
0.250
0.750
Y
X
Z

(b)

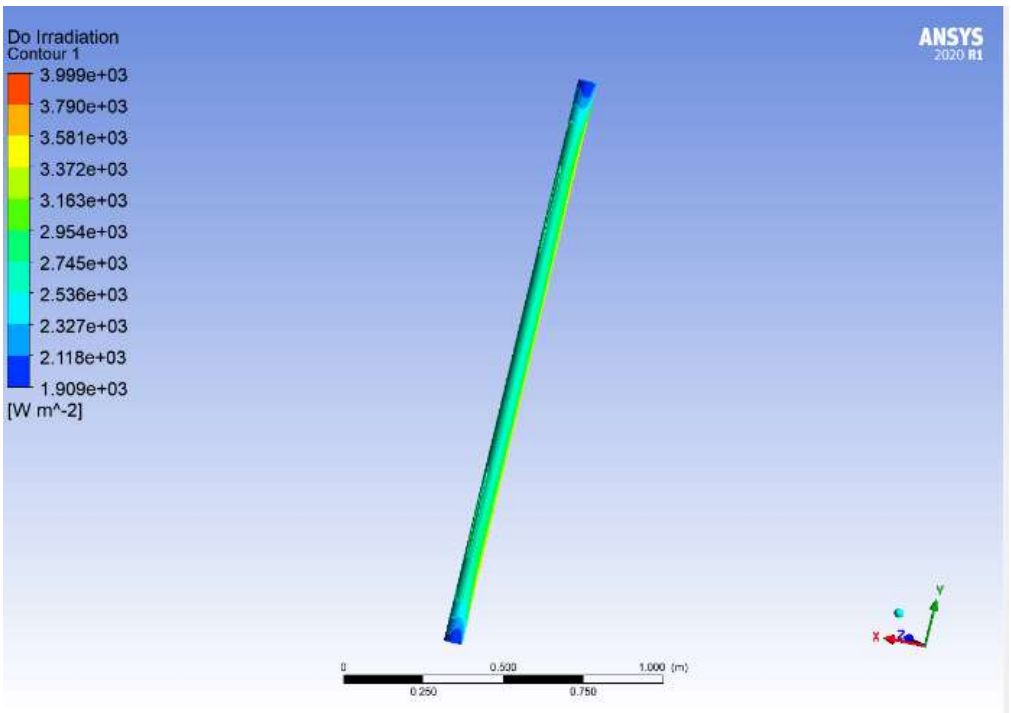
Do Irradiation
Contour 1
3.999e+03
3.790e+03
3.581e+03
3.372e+03
3.163e+03
2.954e+03
2.745e+03
2.536e+03
2.327e+03
2.118e+03
1.909e+03
[W m^-2]
ANSYS
2020 R1
0
0.500
1.000 (m)
0.250
0.750
Y
X
Z

(c)

Figure (14) Focusing solar radiation on the solar collector without tracking system, (a) on parabolic plate, (b) front of tube, (c) back of tube.

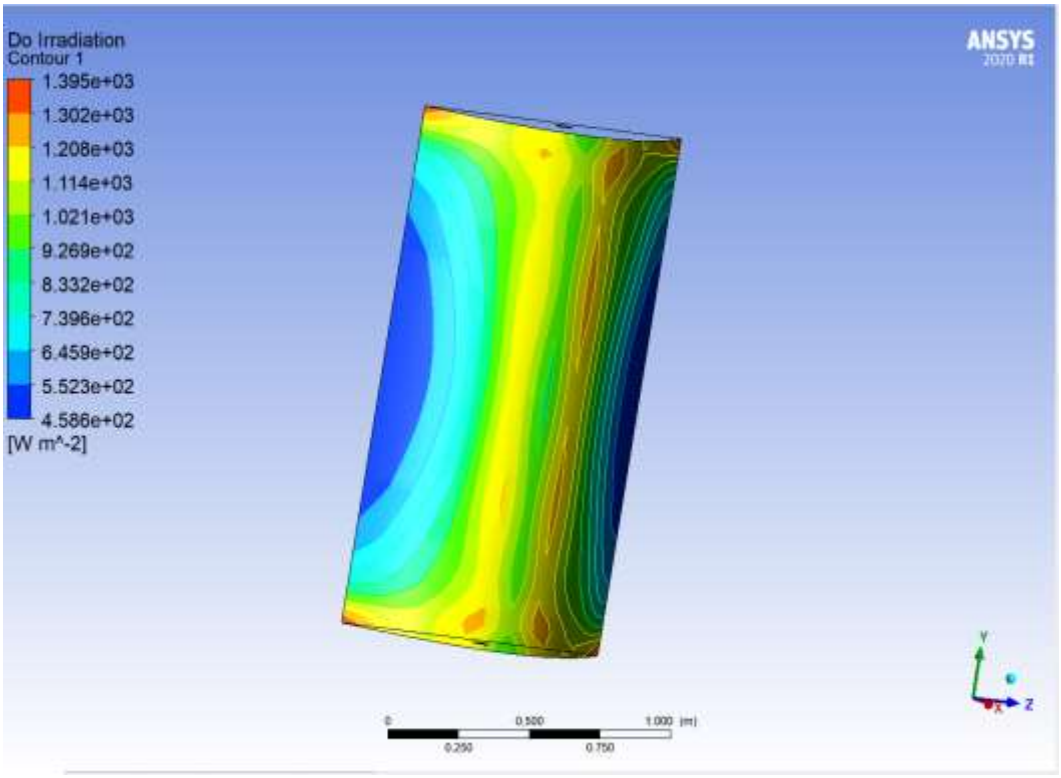

(a)

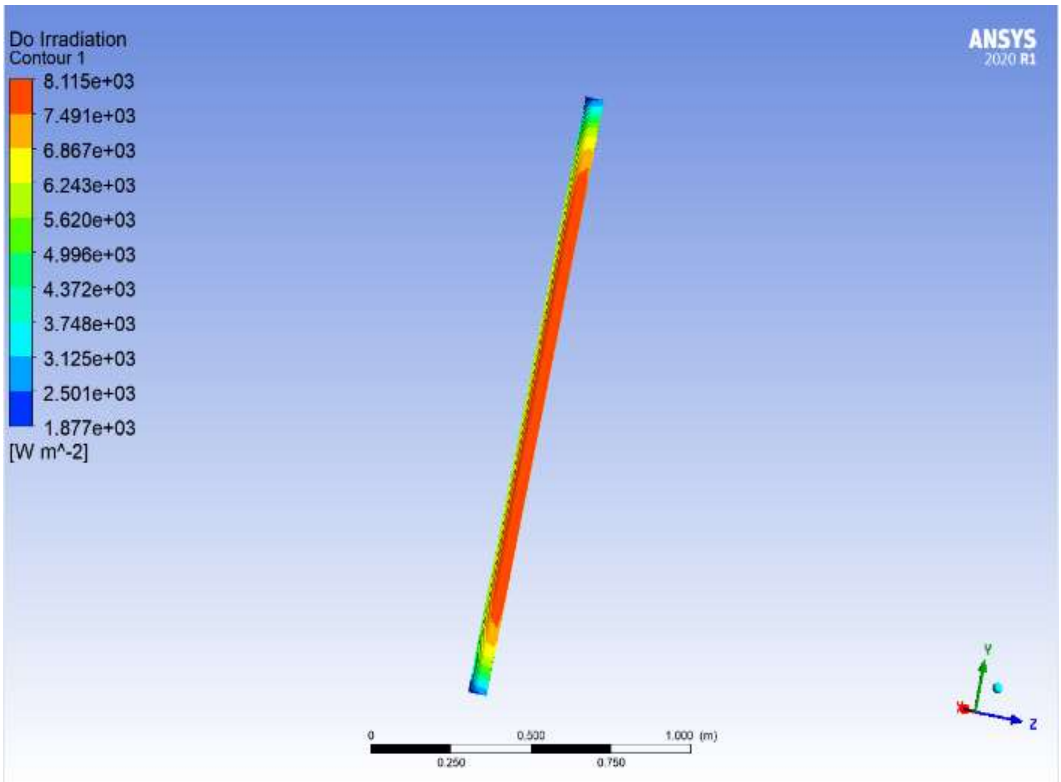

(b)

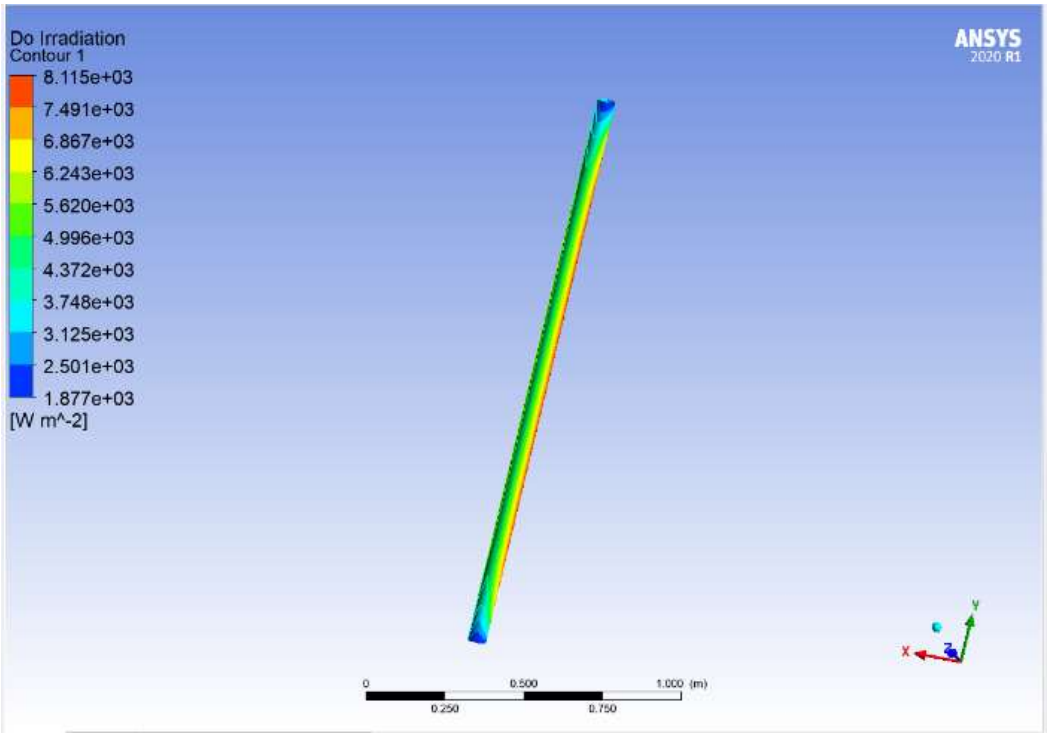

(c)

Figure (15) Focusing solar radiation on the solar collector with tracking system, (a) on parabolic plate, (b) front of tube, (c) back of tube.

It has been noticed from the figures above that the difference in solar radiation in the solar collector is that the radiation value in the solar collector without tracking system is less than the value of the radiation in the solar collector with the presence of the tracking system.

4.Conclusions

Water entering the solar collector obtains the largest amount of thermal energy as a result of the continuous feeding of the solar system from the sun through its movement. The highest temperature in a condition without the tracking system on the first day is 40.5 ^{o}C at 14:30, where the inlet temperature was 25 ^{o}C. Noticed that the highest temperature recorded on the second day has increased to 58 ^{o}C at 14:30. The main work of the solar collector is to reflect the incoming solar radiation onto the tube in which the water flows and heats it. The amount of thermal energy transmitted by the incident radiation was calculated, the thermal energy was obtained, it was 1672 watts at 13:00 (3/28) by the Solar collector with tracking system. By calculating the concentrated solar energy and its transmission to the heat energy acquired through the working fluid (water) and calculating the energy received by the water from the collector tube from the incoming and outgoing temperatures and the amount of flow. Deduce the effectiveness of the tracking system which obtained more thermal energy compared to the solar collector with tracking.

References

1. Limon, D., Alvarado, I., Alamo, T., Ruiz, M., & Camacho, E. (2008). Robust control of the distributed solar collector field ACUREX using MPC for tracking. IFAC Proceedings Volumes, 41(2), 958-963. doi:10.3182/20080706-5-kr-1001.00164.

2. Limon, D., Alvarado, I., Alamo, T., Ruiz, M., & Camacho, E. (2008). Robust control of the distributed solar collector field ACUREX using MPC for tracking. IFAC Proceedings Volumes, 41(2), 958-963. doi:10.3182/20080706-5-kr-1001.00164.

3. Bakos, G. C. (2006). Design and construction of a two-axis Sun tracking system for parabolic trough collector (PTC) efficiency improvement. Renewable Energy, 31(15), 2411-2421. doi: 10.1016/j.renene.2005.11.008.

4. Chong, K., & Wong, C. (2009). General formula for on-axis sun-tracking system and its application in improving tracking accuracy of solar collector. Solar Energy, 83(3), 298-305. doi: 10.1016/j.solener.2008.08.003.

5. Saad D. Odeh. Hosni I. Abu-Mulaweh. Design and development of an educational solar tracking parabolic trough collector system. Global Journal of Engineering Education. Volume 15, Number 1, 2013.

6. Gaspar, Ferenc, et al. "Experimental Study on the Sun Tracking Ability of a Spherical Solar Collector." Energy Procedia, vol. 85, Jan. 2016, pp. 220–227, 10.1016/j.egypro.2015.12.227. Accessed 3 Nov. 2021.

7. Gitan, Ali Ahmed, et al. "Tracking Collector Consideration of Tilted Collector Solar Updraft Tower Power Plant under Malaysia Climate Conditions." Energy, vol. 93, Dec. 2015, pp. 1467–1477, 10.1016/j.energy.2015.09.009. Accessed 3 Nov. 2021.

8. Handoyo, Ekadewi A., et al. "The Optimal Tilt Angle of a Solar Collector." Energy Procedia, vol. 32, 2013, pp. 166–175, 10.1016/j.egypro.2013.05.022. Accessed 3 Nov. 2021.

9. Jalil, Saifuddin, et al. "Design of Maximum Power Point Tracking for Solar Collector Drying System: An Experimental Study." International Journal of Power Electronics and Drive System (IJPEDS), vol. 9, no. 4, 2018, pp. 1799–1803, 10.11591/ijpeds.v9n4.pp1799-1803. Accessed 3 Nov. 2021.

10. Mustafa, Falah, et al. Simple Design and Implementation of Solar Tracking System Two Axis with Four Sensors for Baghdad City.

11. Falah I. Mustafa, Sarmid Shakir. "Simple Design and Implementation of Solar Tracking System Two Axis with Four Sensors for Baghdad City." The 9th International Renewable Energy Congress, 25 Nov. 2013. Accessed 3 Nov. 2021.

12. Odeh, Saad D., and G. L. Morrison. "Optimization of Parabolic Trough Solar Collector System." International Journal of Energy Research, vol. 30, no. 4, 2006, pp. 259–271, 10.1002/er.1153. Accessed 3 Nov. 2021.

13. Qu, Wanjun, et al. "Test of a Solar Parabolic Trough Collector with Rotatable Axis Tracking." Applied Energy, vol. 207, Dec. 2017, pp. 7–17, 10.1016/j.apenergy.2017.05.114. Accessed 3 Nov. 2021.

14. Sallaberry, Fabienne, et al. "Optical Losses due to Tracking Error Estimation for a Low Concentrating Solar Collector." Energy Conversion and Management, vol. 92, Mar. 2015, pp. 194–206, 10.1016/j.enconman.2014.12.026. Accessed 3 Nov. 2021.

15. Zhai, H., et al. "Experimental Investigation and Analysis on a Concentrating Solar Collector Using Linear Fresnel Lens." Energy Conversion and Management, vol. 51, no. 1, Jan. 2010, pp. 48–55, 10.1016/j.enconman.2009.08.018. Accessed 3 Nov. 2021.

16. Zhao, Dongming, et al. "Influences of Installation and Tracking Errors on the Optical Performance of a Solar Parabolic Trough Collector." Renewable Energy, vol. 94, Aug. 2016, pp. 197–212, 10.1016/j.renene.2016.03.036. Accessed 3 Nov. 2021.